Inhibition of Type I and Type II Phosphomannose Isomerases by the Reaction Intermediate Analogue 5-Phospho-D-Arabinonohydroxamic Acid Supports a Catalytic Role for the Metal Cofactor†

Céline Roux,‡ Ji Hyun Lee,§ Constance J. Jeffery,§ and Laurent Salmon*,‡

Laboratoire de Chimie Bioorganique et Bioinorganique, Centre National de la Recherche Scientifique, Unité Mixte de Recherche 8124, Institut de Chimie Moléculaire et des Matériaux d'Orsay, Bâtiment 420, Université Paris-Sud XI, 91405 Orsay, France, and Laboratory for Molecular Biology, MC567, Department of Biological Sciences, University of Illinois, Chicago, Illinois 60607

Received September 18, 2003; Revised Manuscript Received November 24, 2003

ABSTRACT: The phosphomannose isomerases (PMI) comprise three families of proteins: type I, type II, and type III PMIs. Members of all three families catalyze the reversible isomerization of D-mannose 6-phosphate (M6P) and D-fructose 6-phosphate (F6P) but share little or no sequence identity. Because (1) PMIs are essential for the survival of several microorganisms, including yeasts and bacteria, and (2) the PMI enzymes from several pathogens do not share significant sequence identity to the human protein, PMIs have been considered as potential therapeutic targets. Elucidation of the catalytic and regulatory mechanisms of the different types of PMIs is strongly needed for rational species-specific drug design. To date, inhibition and crystallographic studies of all PMIs are still largely unexplored. As part of our research program on aldose−ketose isomerases, we report in this paper the evaluation of two new inhibitors of type I and type II PMIs from baker's yeast and *Pseudomonas aeruginosa*, respectively. We found that 5-phospho-D-arabinonohydroxamic acid (5PAH), which is the most potent inhibitor of phosphoglucose isomerase (PGI), is by far the best inhibitor ever reported of both type I and type II PMI-catalyzed isomerization of M6P to F6P. 5PAH, which has an inhibition constant at least 3 orders of magnitude smaller than that of previously reported PMI inhibitors, may be the first high-energy intermediate analogue inhibitor of the enzymes. We also tested the related molecule 5-phospho-D-arabinonate (5PAA), which is a strong competitive inhibitor of PGI, and found that it does not inhibit either PMI. All together, our results are consistent with a catalytic role for the metal cofactor in PMI activity.

Originally discovered from baker's yeast in 1950 (*1*), phosphomannose isomerase (PMI,[1] EC 5.3.1.8) catalyzes the reversible isomerization of D-mannose 6-phosphate (M6P) and D-fructose 6-phosphate (F6P; Figure 1), with a high specificity for the β-anomer of each substrate (*2*−*4*). In all eukaryotes and prokaryotes investigated so far, the enzyme has been reported to play a crucial role in both D-mannose metabolism and the supply of the activated mannose donor guanosine diphosphate D-mannose (GDP-D-mannose), which is a required reactant for the biosynthesis of many mannosylated structures, including glycoproteins, glycolipids, and, in the case of microorganisms such as fungi, cell wall components. In addition, GDP-D-mannose is a precursor for other activated nucleotide sugars that are also involved in the synthesis of various glycoconjugates. Following PMI-catalyzed isomerization of F6P to M6P and subsequent conversion of M6P to D-mannose 1-phosphate (M1P) by phosphomannomutase (PMM), incorporation of GTP by GDP-D-mannose pyrophosphorylase (GMP) yields GDP-D-mannose (Figure 2).

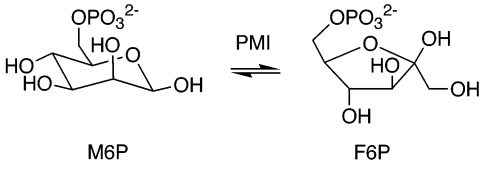

FIGURE 1: Reversible interconversion of F6P and M6P catalyzed by phosphomannose isomerases. Only the β-pyranose anomers are reported to be substrates of the enzymes (*3*).

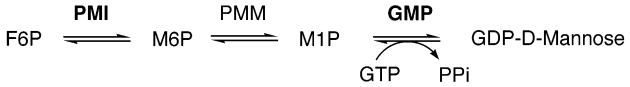

FIGURE 2: GDP-D-mannose biosynthesis pathway from F6P. The PMI and GMP activities of type II PMIs are indicated in bold letters.

PMIs are considered to be potential therapeutic targets because of their role in survival and pathogenesis in several microbes, and in many cases, there are significant differences

† This research was supported in part by a grant from the American Heart Association to CJJ.

* To whom correspondence should be addressed. Tel: +33 1 69 15 63 11. Fax: +33 1 69 15 72 81. E-mail: lasalmon.icmo.u-psud.fr.

‡ Université Paris-Sud XI.

§ University of Illinois.

[1] Abbreviations: 5PAA, 5-phospho-D-arabinonate; 5PAH, 5-phospho-D-arabinonohydroxamic acid; CF, cystic fibrosis; F6P, D-fructose 6-phosphate; G6P, D-glucose 6-phosphate; GDP, guanosine diphosphate; GMP, GDP-D-mannose pyrophosphorylase; GTP, guanosine triphosphate; G6PDH, D-glucose-6-phosphate dehydrogenase; HEPES, *N*-(2-hydroxyethyl)piperazine-*N*′-2-ethanesulfonic acid; M1P, D-mannose 1-phosphate; M6P, D-mannose 6-phosphate; PDB, Protein Data Bank; PGI, phosphoglucose isomerase; PMI, phosphomannose isomerase; PMM, phosphomannomutase; TBA, thiobarbituric acid.

10.1021/bi035688h CCC: $27.50
Published on Web 02/17/2004

in amino acid sequence between the PMIs from pathogens and humans. Indeed, unless the growth medium is supplemented with D-mannose, PMI has been found to be essential for the survival of cells from *Saccharomyces cerevisiae* (*5*), *Candida albicans* (*6*), and *Mycobacterium smegmatis* (*7*) and important for the virulence of the protozoan parasite *Leishmania mexicana* (*8*). PMI is also needed for the development of mucoid strains of *Pseudomonas aeruginosa* that cause recurrent and life-threatening lung infections in cystic fibrosis (CF) patients. The serious lung infections are a major cause of the decreased life expectancy of CF patients. PMI has been found to be essential in the production of the exopolysaccharide alginate (*9*), which coats the bacteria and protects them from antibiotics and the host's immune system.

In most human tissues, the bulk of the central metabolite M6P that is utilized for glycoprotein synthesis is likely not derived from G6P but originates from efficient uptake of D-mannose in serum through a specific mannose transporter, followed by phosphorylation by hexokinase (*10*). In humans, a deficiency of PMI activity leads to carbohydrate-deficient glycoprotein syndrome type 1b (CGDS 1b), a severe metabolic disorder with hepatic−intestinal presentation (*11*, *12*), that is however today successfully treated by oral D-mannose (*13*).

From sequence alignments and physicochemical and kinetic characterization, a classification of PMIs has been proposed by Proudfoot et al. (*14*). Type I PMIs, which include proteins from *Aspergillus nidulans*, *C. albicans*, *Escherichia coli*, *Homo sapiens*, *Salmonella enterica*, *S. cerevisiae* (*15*, *16*), *Caenorhabditis elegans*, *Streptococcus mutans* (*17*), and *Cryptococcus neoformans* (*18*), are homologous monofunctional enzymes catalyzing the single isomerization reaction. The type I PMI isolated from *S. cerevisiae* in 1968 (*19*) has been shown to be a zinc-dependent metalloenzyme, with one metal atom per molecule of the 45 kDa monomer (*20*). A high-resolution X-ray crystal structure of the type I PMI from *C. albicans* is the only 3D structure of a PMI reported to date (*21*). A pocket on the surface that is very likely to be the active site and a zinc metal cofactor binding site have been identified; however, the roles of the individual active site amino acids and zinc ion in the catalytic mechanism are still not known.

Type II PMIs are bifunctional enzymes possessing both PMI and GMP activities (Figure 2) in separate catalytic domains. In some species the PMI and GMP domains are found as separate proteins (*17*). Type II PMIs reported so far are found only in some bacteria, including *P. aeruginosa* (*9*), *Xanthomas campestris* (*22*), *Acinetobacter calcoaceticus* (*17*), *Rhodospirillum rubrum* (*23*), *Acetobacter xylinum* (*24*), *Salmonella typhimurium* (*25*, *26*), and *Helicobacter pylori* (*27*). A recently reported sequence alignment and database search reveals that all type II PMI/GMP bifunctional proteins share a high degree of sequence identity and contain three highly conserved amino acid sequence motifs. PMI activity in type II enzymes uses Zn^{2+} as the metal cofactor but also can use other divalent cations, Co^{2+}, Mg^{2+}, Mn^{2+}, Ca^{2+}, or Ni^{2+}, depending on the enzyme source. The PMI domain of the bifunctional enzymes still conserves the zinc binding amino acid motif QXH also seen in zinc metalloenzymes, although the reason the PMI domain is not specific for Zn^{2+} has not been elucidated (*27*). So far, only one type III PMI has been reported, from *Rhizobium meliloti* (*28*).

Due to the level of amino acid sequence identity (>40%) among type I PMIs from pathogenic microorganisms such as bacteria, yeasts, and *H. sapiens*, it appears that it might be difficult to achieve species-specific inhibition of a fungal or bacterial type I PMI. On the other hand, no sequence identity is found between type I and type II enzymes, except for a very small conserved amino acid sequence motif, which makes up part of the active site in the crystal structure (*17*). Therefore, specific inhibition of the PMI activity, while leaving the human type I protein unaffected, should be achieved more easily for type II than for type I pathogenic proteins (*27*). This suggests the possibility of rational design of potent and highly species-specific inhibitors against the targeted PMIs from pathogens.

As matters stand, elucidation of the catalytic and regulatory mechanisms of type I and type II PMIs is strongly needed for rational drug design. To date, inhibition and crystallographic studies of all PMIs are still largely unexplored. Hence, as part of our program of study of aldose−ketose isomerases, we report in this paper a potent competitive inhibitor for isomerization of M6P to F6P by both type I (*S. cerevisiae*) and type II (*P. aeruginosa*) enzymes. The competitive inhibitor, designed as an analogue of the postulated high-energy intermediate, is by far the strongest ever evaluated on a PMI, with inhibition constant values in the nanomolar range. In addition, further inhibition studies on both PMIs and comparison to kinetic studies of phosphoglucose isomerase are consistent with a catalytic role for the metal cofactor.

MATERIALS AND METHODS

Materials. The disodium salt of 5-phospho-D-arabinonohydroxamic acid and the trisodium salt of 5-phospho-D-arabinonate were synthesized according to the reported procedures (*29*−*31*). M6P was purchased as the barium salt and converted to the sodium salt by ion-exchange chromatography with a Dowex-50X4−400 resin. PMI from *P. aeruginosa* was overexpressed and purified as previously described (*9*, *32*). Purified water (18.2 MΩ), used for the preparation of the buffer, was obtained by filtration through a Milli-Q device (0.22 μm) from Millipore. All other commercial chemicals and biochemicals were of reagent grade from Sigma-Aldrich Chemical Co. and were used without further purification. All solutions and enzyme aliquots were stored at −20 °C, except the buffer solution, which was stored at 4 °C, and the $NADP^+$ solution, which was freshly prepared prior to use.

Instruments. UV absorbance measurements were made with a Safas 190 DES spectrophotometer equipped with a Julabo thermostat regulation device, using 1 mL of Brand polystyrene disposable cuvettes of 1 cm optical path.

PMI Assays Using the PGI/G6PDH Coupled Enzyme Method. Yeast and *P. aeruginosa* PMI activities were spectrophotometrically assayed at 340 nm using a coupled enzyme assay with PMI activity coupled to the activities of yeast PGI and yeast D-glucose-6-phosphate dehydrogenase (G6PDH), following a procedure adapted from the literature (*19*, *33*). Both auxiliary enzymes were added in excess so that the rate-limiting reaction was the PMI-catalyzed isomerization of M6P to F6P. Careful control experiments were conducted to check this assumption by adding further excess

of the auxiliary enzymes in the presence of the inhibitor at its highest concentration. In some cases, this enzymatic assay could not be used for the PMI assays, so instead the colorimetric assay described below was employed. The activity measurements were made using the multicuvette mode with the temperature held at 25 °C. Specific activities were measured using a substrate concentration of at least 5 times the corresponding K_m value. In the case of yeast PMI, the assay mixture contained, in a volume of 1 mL, 50 mM HEPES buffer, pH 7.1, previously sterilized and filtered (0.22 μm), 0.05−2 mM M6P sodium salt (100 mM in buffer), 5 mM $MgCl_2$ (500 mM aqueous solution), 0.4 mM $NADP^+$ sodium salt (40 mM in buffer, used up to 2 weeks after preparation), 0.63 unit of G6PDH (6 mg of lyophilized protein in 816 μL of water; a 10 μL aliquot was diluted to 100 μL with buffer just prior to use), and 0.6 unit of PGI (2 mg of lyophilized protein in 500 μL of water and dilution prior to use of a 10 μL aliquot to 100 μL with buffer). The 5PAH inhibitor was included at final concentrations of 0−0.25 μM 5PAH (100 mM aqueous solution appropriately diluted 10, 100, or 1000 times). Following preincubation in the spectrophotometer compartment until no further increase in absorbance due to substrate occurred (6−7 min), the reaction was initiated by the addition of 0.006 unit of PMI (32.5 μL of commercial solution diluted to 100 μL with buffer and further dilution of a 5 μL aliquot to 500 μL with buffer prior to use). In the case of *P. aeruginosa* PMI, the enzymatic assay was identical except for the following values: 0.4−3.5 mM M6P, 6.3 units of G6PDH, 6.0 units of PGI, and 0.006 unit of PMI. The 5PAH inhibitor was included at final concentrations of 0−0.8 μM 5PAH. The rate of absorbance change due to NADPH formation (ϵ = 6220 M^{-1} cm^{-1}) coupled to M6P isomerization was then measured. PGI activity was assayed analogously with F6P as described elsewhere (*34*, *35*), as well as G6PDH with G6P. Triplicate kinetic data were analyzed by double reciprocal plots of the initial reaction velocity versus M6P concentration measured at various inhibitor concentrations. Nonlinear least-squares fit to the observed data using the Michaëlis−Menten equation for competitive inhibition allowed secondary graphical representation of the slope as a function of inhibitor concentration, from which was obtained the value of the inhibition constant (K_i). Units of enzyme activity are defined as micromoles of substrate converted per minute at 25 °C under the assay conditions described.

PMI Assays Using the TBA Colorimetric Method. Yeast and *P. aeruginosa* PMI activities were spectrophotometrically assayed using the thiobarbituric acid (TBA) colorimetric method adapted from the procedures first reported by Percheron (*36*) and Zender and co-workers (*37*). In the case of yeast PMI, the assayed mixture contained, in a final volume of 1 mL, 50 mM HEPES buffer, pH 7.1, 0.2 mM M6P (a concentration close to the K_m value was chosen), and 5 mM $MgCl_2$. Inhibitors were used at the following concentrations: 5PAH at 0−150 nM or 5PAA at 0−15 mM. Following preincubation at 25 °C for 15 min, the reaction was initiated by the addition of 0.006 unit of PMI. Precisely 5 min later (initial rate conditions), the reaction was stopped by the addition of 2 mL of a 0.01 M thiobarbituric acid solution in concentrated HCl (prepared daily), yielding a total volume of 3 mL. After being heated to 80 °C for 6 min, the reaction mixture was cooled to room temperature in an ice−water bath and under running water. After the reaction was stopped with TBA (90 min), the amount of F6P formed was measured from the absorbance of the TBA adduct at 434 nm [ϵ measured = (53 ± 2) × 10^3 M^{-1} cm^{-1}]. Graphical representation of the initial rate of formation of F6P as a function of the inhibitor concentration allowed the determination of the IC_{50} value (inhibitor concentration that gives an initial rate equal to 50% of the rate in the absence of inhibitor). In the case of *P. aeruginosa* PMI, the colorimetric assay was identical except for the following reagent and inhibitor concentrations: 2.5 mM M6P and 5PAH at 0−500 nM or 5PAA at 0−20 mM.

Table 1: Inhibition by 5PAH and 5PAA of the M6P to F6P Isomerization Catalyzed by Yeast and *P. aeruginosa* PMIs

inhibitor	parameter	yeast PMI[a]	*P. aeruginosa* PMI[b]
none	K_m (mM)[c]	0.121 ± 0.013	2.5 ± 0.2
	k_{cat} (s^{-1})[c]	20 ± 2	0.076 ± 0.005
	k_{cat}/K_m (mM^{-1} s^{-1})[c]	165 ± 34	0.030 ± 0.004
5PAH	K_i (μM)[c]	0.086 ± 0.015	0.137 ± 0.012
	K_m/K_i[c]	1410	18250
	IC_{50} (μM)[d]	0.136 ± 0.008	0.169 ± 0.014
5PAA	IC_{50} (mM)[d]	3.6 ± 0.7	20 ± 1

[a] Specific activity = (48 ± 3) × 10^{-5} unit μL^{-1}. [b] Specific activity = (9.3 ± 0.7) × 10^{-5} unit μL^{-1}. [c] Using the PGI/G6PDH coupled enzyme assay. [d] Using the TBA colorimetric assay. See Materials and Methods for details on kinetic assay conditions.

RESULTS

Kinetic Parameters of Type I and Type II PMIs. The values of K_m, k_{cat}, and k_{cat}/K_m for the M6P to F6P isomerization reaction were measured for both commercial yPMI and recombinantly expressed and purified PaPMI and are reported in Table 1. Considering the different conditions used for the kinetics assays, the K_m values of 0.12 and 2.5 mM we determined for yPMI and PaPMI, respectively, are in the range of those previously reported, 0.65 mM (*15*) and 3.03 mM (*9*), respectively. Also, comparison of the k_{cat}/K_m parameters indicates that type I yPMI is a much more efficient catalyst than type II PaPMI for the reaction in the M6P to F6P direction. This is consistent with the fact that the two enzymes catalyze the reaction in different directions in their respective biochemical pathways. yPMI catalyzes the reaction in the M6P to F6P direction for M6P utilization. PaPMI catalyzes the reaction in the F6P to M6P direction in the alginate biosynthesis pathway. It has been suggested that PaPMI has evolved to be well suited for alginate production, not for D-mannose utilization (*9*).

Design of the Inhibitors. On the basis of biochemical characterization of PMI, including isotopic exchange studies (*15*, *38*) and affinity labeling and mutagenesis (*39*, *40*), the reversible isomerization mechanism of M6P to F6P (Figure 1) has been proposed to involve proton transfer between carbon atoms C2 and C1 and between oxygen atoms O2 and O1. Thus, the mechanism for interconversion of F6P and M6P by PMI shares important similarities with the mechanism for the interconversion of G6P and F6P by PGI. However, there are also important differences: (i) PMI requires the presence of a metal cofactor at the active site for activity, and (ii) the *pro-S* hydrogen of F6P is transferred in PMI, while it is the *pro-R* hydrogen in PGI (*41*). Nevertheless, both enzyme mechanisms may very likely

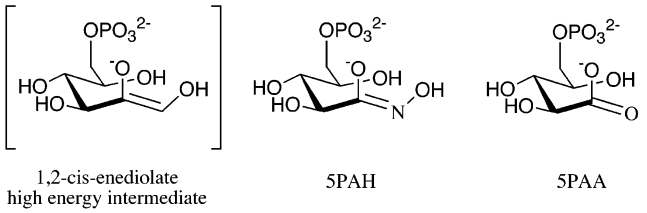

FIGURE 3: Postulated 1,2-*cis*-enediolate high-energy intermediate (HEI) thought to be involved in the reversible isomerization of M6P to F6P catalyzed by PMIs and the two HEI analogue inhibitors evaluated: 5-phospho-D-arabinonohydroxamic acid (5PAH, here depicted as its basic hydroximate form) and 5-phospho-D-arabinonate (5PAA).

involve an identical 1,2-*cis*-enediol (or 1,2-*cis*-enediolate) high-energy intermediate (HEI) (*38*). Although several competitive inhibitors reported in the literature were evaluated on PMIs from various sources, including 4-phospho-D-erythrose (*14*, *42*), 5-phosphate-D-arabinose (*14*), and 1-phosphate-D-fructose (*43*), none of them displayed a K_i value lower than 40 μM or a K_m/K_i ratio higher than 15, so no PMI inhibitor reported to date can be considered to be a good high-energy intermediate or transition state analogue inhibitor. Consequently, we selected 5-phospho-D-arabinonohydroxamic acid (5PAH) and 5-phospho-D-arabinonate (5PAA), the two most efficient inhibitors of PGI reported in the literature (*29*, *30*, *35*, *44*), as good candidates for strong inhibition of the PMI-catalyzed isomerization of M6P to F6P (Figure 3). The two PGI inhibitors were evaluated on both the type I PMI from *S. cerevisiae* (yPMI), which is commercially available, and the type II PMI from *P. aeruginosa* (PaPMI), which was recombinantly expressed and purified (*9*, *32*). Enzyme activity was measured according to two different procedures adapted from the literature as described in Materials and Methods: (i) the PGI/G6PDH coupled enzyme method (*33*) for determinations of the K_i in the case of 5PAH and (ii) the thiobarbituric acid colorimetric (TBA) method (*36*, *37*) for determinations of the IC_{50} for both 5PAH and 5PAA. Results of these inhibition studies are reported in Table 1.

Inhibition of PMIs by 5PAH. In the case of 5PAH, double reciprocal plots of initial reaction velocity versus substrate (M6P) concentrations obtained with various concentrations of the inhibitor are depicted in Figure 4 for (a) yPMI and (b) PaPMI. 5PAH appears to be a strong competitive inhibitor of both enzymes with K_i values of 86 and 137 nM (Table 1), respectively, overwhelming reported inhibition constants of known PMIs inhibitors by about 3 orders of magnitude. While not conclusive, values of 1410 and 18250, respectively, for the calculated binding ratio K_m/K_i are consistent with 5PAH behaving as a stable high-energy (or activated) intermediate analogue inhibitor of the M6P to F6P isomerization reaction. Our two reported K_i values for 5PAH are in the same range for both the type I and type II enzymes. However, the higher K_m value for M6P with PaPMI than with yPMI (2.5 vs 0.12 mM, respectively) results in a higher K_m/K_i ratio that shows that inhibition of the M6P to F6P isomerization by 5PAH affects more specifically the type II than the type I enzyme (Table 1).

Because PGI, which is one of the coupled enzymes involved in the enzymatic procedure used for the determination of PMI activity, is known to be strongly inhibited by 5PAH (*30*), we used a 100-fold excess (in units) of the

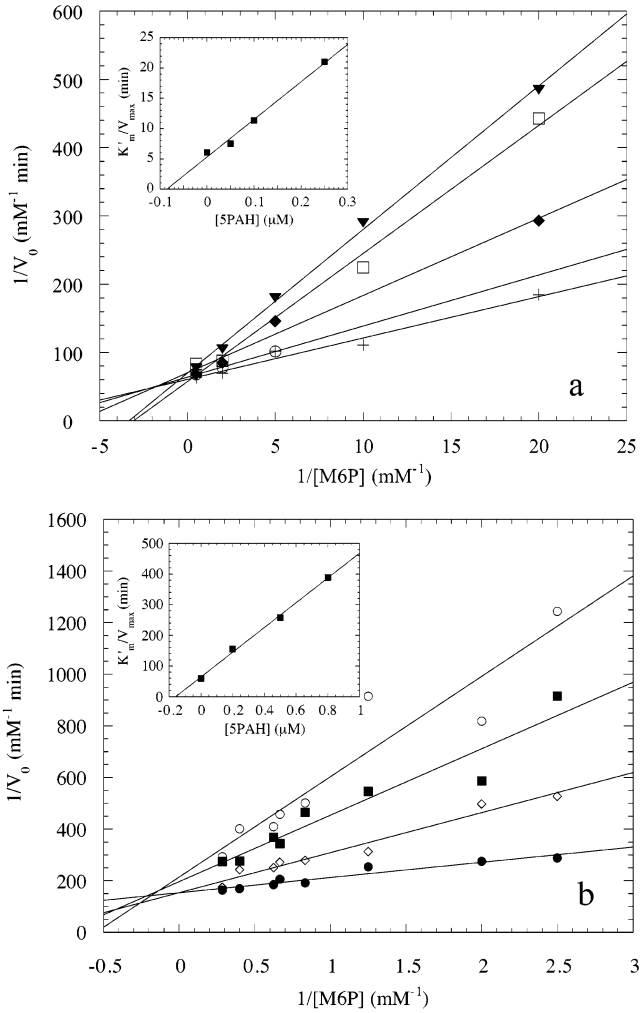

FIGURE 4: Inhibition of PMIs from (a) yeast and (b) *P. aeruginosa* by the high-energy intermediate analogue 5-phospho-D-arabinonohydroxamic acid (5PAH) using the PGI/G6PDH coupled enzyme assay method (see Materials and Methods for details on kinetic assay conditions). Double reciprocal plot of the initial reaction velocity versus M6P concentration obtained at various concentrations of inhibitor 5PAH: (a) (+) no inhibitor, (○) [I] = 0.05 μM, (◆) [I] = 0.10 μM, (□) [I] = 0.15 μM, and (▼) [I] = 0.20 μM; (b) (●) no inhibitor, (◇) [I] = 0.20 μM, (■) [I] = 0.50 μM, and (○) [I] = 0.80 μM. In the inserted secondary plot, the values of the slopes (K'_m/V_{max}) of the straight lines in the primary graphs were plotted against the inhibitor concentrations, which gives $-K_i$ for the intercept.

coupled enzymes PGI and G6PDH (about 0.6 unit). In addition, we carefully performed control experiments designed to check that the PMI-catalyzed step was indeed the one inhibited by 5PAH or, in other words, that the PMI step was rate-determining, even at the highest inhibitor concentration employed (0.3 μM). As shown in Figure 5, yPMI activity increases linearly upon use of 5 and 10 equiv of enzyme units, while yPMI activity does not change upon use of 5 and 10 equiv of PGI or G6PDH units. This graph proves that, in the conditions we used, neither PGI or G6PDH is significantly inhibited by 5PAH with respect to the inhibition of PMI. The K_i values we determined for 5PAH were further confirmed through the use of the TBA colorimetric assay, which gave us IC_{50} values in the same range, i.e., 136 and 169 nM for yPMI and PaPMI, respectively. This colorimetric method allowed us to determine PMI activity by quantitative analysis of the amount of F6P produced as a function of

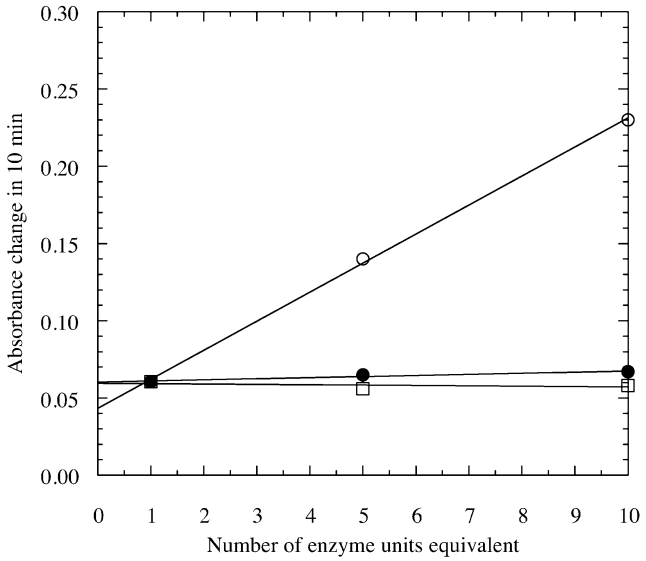

FIGURE 5: Control experiments for the inhibition assays of the yPMI-catalyzed isomerization of M6P (0.1 mM) to F6P by 5PAH (0.3 μM). Increasing numbers of enzyme unit equivalents were used: (○) PMI (0.006, 0.03, and 0.06 unit, using 0.6 unit of PGI and 0.63 unit of G6PDH), (●) PGI (0.6, 3, and 6 units, using 0.006 unit of PMI and 0.63 unit of G6PDH), and (□) G6PDH (0.6, 3, and 6 units, using 0.006 unit of PMI and 0.6 unit of PGI).

time and without the use of any coupled enzyme, notably PGI. The method, which we have adapted from the literature (see Materials and Methods for details), was first reported by Percheron in 1962 for the quantitative analysis of fructose and fructofuranosides (*36*) and was thereafter improved by Zender and co-workers for the analysis of the fructose and insulin levels in plasma and urine (*37*). Finally, we have performed a theoretical study of the inhibition of only the enzyme PGI by 5PAH according to the equation:

$$[EI]^2 - (K_i + [E]_0 + [I]_0)[EI] + [E]_0[I]_0 = 0 \quad (1)$$

Knowing the K_i value of 5PAH on yeast PGI [200 nM (*30*)] and the initial concentration of the enzyme in the conditions used for the yPMI and PaPMI kinetic assays ($[E]_0 = 18$ and 180 nM, respectively), eqs 2−4 allow us to plot the calculated fractions of the PGI−5PAH Michaëlis complex ($[EI]/[E]_0$), free 5PAH ($[I]/[I]_0$), and free PGI ($[E]/[E]_0$) as a function of the initial concentration of 5PAH ($[I]_0$) as represented in Figure 6. At the highest 5PAH concentration

$$[EI] = {}^1/_2(K_i + [E]_0 + [I]_0 - \sqrt{(K_i + [E]_0 + [I]_0)^2 - 4[E]_0[I]_0}) \quad (2)$$

$$[I] = [I]_0 - [EI] \quad (3)$$

$$[E] = [E]_0 - [EI] \quad (4)$$

used (300 nM) in our inhibition studies of PMIs using the coupled enzyme assay, Figure 6 shows that free PGI accounts for about 41% (yPMI) and 49% (PaPMI) of the initial PGI concentration, which means that the activity of free PGI is still in 41- and 490-fold excess of the amount of yPMI and PaPMI, respectively. Also, the fractions of free 5PAH are 97% and 70% of the initial concentration, respectively. Accordingly, Figure 7 shows the secondary graphical representations of the slope K_m'/V_{max} (previously determined

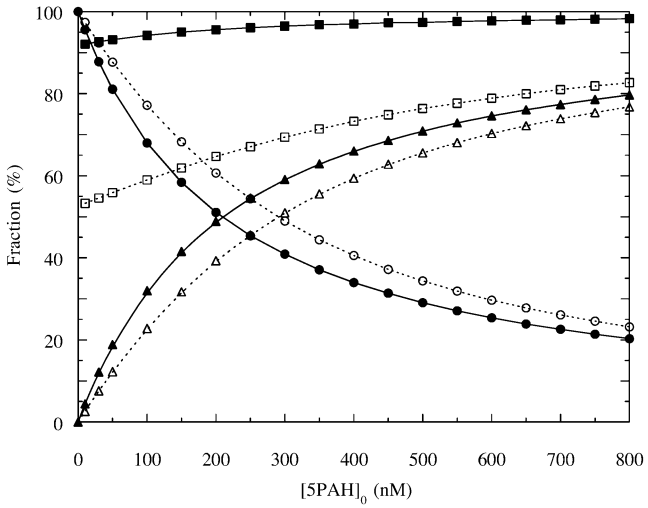

FIGURE 6: Calculated fractions of the PGI−5PAH Michaëlis complex (▲, △), free 5PAH (■, □), and free PGI (●, ○) as a function of the initial concentration of the inhibitor ($[5PAH]_0$) for the enzymatic evaluation of yPMI (filled symbols) and PaPMI (empty symbols) activities.

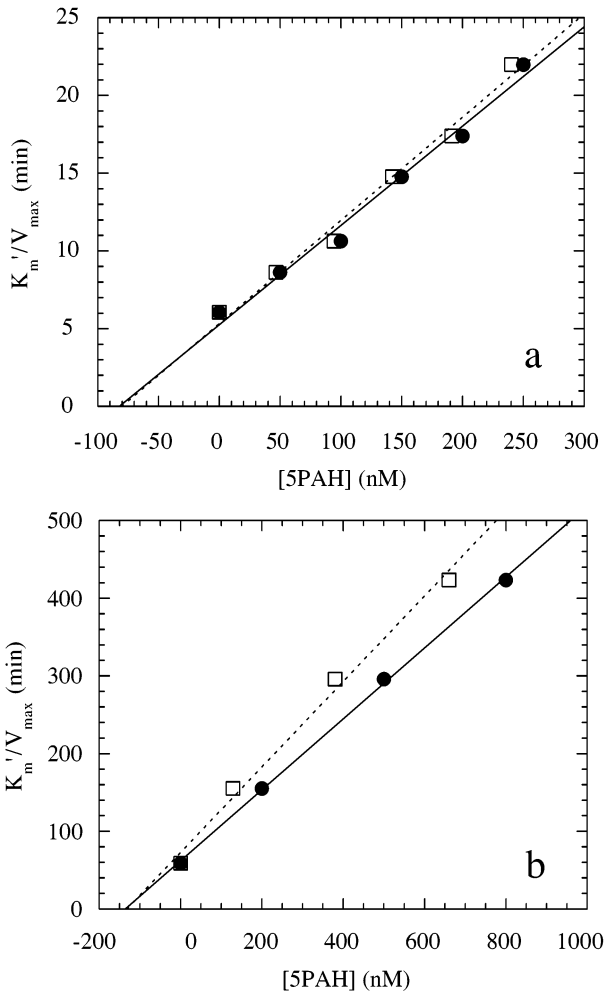

FIGURE 7: Graphical determinations of the K_i values for the inhibition of (a) yPMI and (b) PaPMI by 5PAH using uncorrected (●) and corrected (□) values of the inhibitor concentrations.

from the corresponding Lineweaver−Burk primary graphs) as a function of the uncorrected (or initial) and corrected 5PAH concentration for both yPMI (Figure 7a) and PaPMI (Figure 7b) activity measurements. In both cases, the same

K_i value is obtained from the intercept whether uncorrected or corrected 5PAH concentrations are used, further confirming the validity of the conditions we used in our kinetic assays using the coupled PGI/G6PDH method.

PMI Inhibition by 5PAA. The results of inhibition studies with 5PAA are quite different from the results with 5PAH on both yPMI and PaPMI. In constrast to 5PAH, the respective IC_{50} values of 3.6 and 20 mM we obtained (Table 1) indicate that 5PAA is surprisingly not an inhibitor of either PMI studied.

DISCUSSION

In this inhibition study of type I yPMI and type II PaPMI, we have found 5PAH (Figure 3) to be the most potent competitive inhibitor of the M6P to F6P isomerization reaction catalyzed by a PMI (Figure 1) ever reported in the literature, with K_i values in the submicromolar range (Table 1). While the value of the binding ratio K_m/K_i itself does not prove an inhibitor to be a high-energy intermediate (or a transition state) analogue inhibitor, our results are consistent with the hypothesis that 5PAH may behave as such. Indeed, other hydroxamate inhibitors considered to be high-energy intermediate analogue inhibitors of the corresponding aldose−ketose isomerizations were reported in the literature; binding ratios of 155 (triosephosphate isomerase) (*45*), 513 (phosphoglucose isomerase) (*30*), and 50000 (xylose isomerase) (*46*) were reported for phosphoglycolohydroxamate versus dihydroxyacetone phosphate, 5PAH versus F6P, and threonohydroxamate versus xylose, respectively. The PMIs' strict specificity for M6P (or F6P) prevents an analysis of the K_m/k_{cat} values for additional substrates and the K_i values of the corresponding hydroxamate analogues that might enable us to more conclusively state the nature of the PMI inhibitor 5PAH, as was done in the case of the phosphoramidate transition state analogue inhibitors of thermolysin (*47*). However, because 5PAH is also the strongest known inhibitor of the analogous G6P to F6P isomerization reaction catalyzed by PGIs (*30*), our results strongly support the model that both the PMI and PGI isomerization mechanisms involve an identical 1,2-*cis*-enediol(ate) high-energy reaction intermediate.

The close similarity of K_i values obtained for both PMIs for 5PAH and 5PAA suggests that the type I and type II active sites for the M6P to F6P isomerization reaction share some structural similarity. This result is surprising since sequence alignments and database searches reported in the literature show that the PMI domain of the type II bifunctional enzymes shares no sequence identity with type I proteins, except for a very short consensus sequence of nine amino acids. The amino acids in this consensus sequence make up a small part of the active site of the type I *C. albicans* PMI crystal structure (*17*, *21*, *27*). At the same time, the K_m/K_i ratios reported in Table 1 favor 5PAH versus M6P binding to type II PaPMI more than to type I yPMI by about 1 order of magnitude. However, from a physiological point of view, the above results might not be prohibitive for the identification of a species-specific inhibitor of PaPMI versus type I human PMI if it is confirmed that the type II enzyme is mainly involved in the reverse conversion of F6P to M6P (*9*). Obviously, 5PAH would also have to be evaluated on type I and type II PMI-catalyzed isomerization of F6P to M6P. To our knowledge, no enzymatic assay that would allow the measurement of PMI activity in the F6P to M6P direction has yet been reported in the literature. Development of such a new enzymatic assay could be soon under investigation in the laboratory.

The fact that 5PAA is not an inhibitor of the M6P to F6P isomerization reaction catalyzed by either PMI is perhaps the most significant finding of our study. This very surprising but interesting result contrasts to the case of PGI where 5PAA is a known strong competitive inhibitor (*29*). At the same time, 5PAH is a strong competitive inhibitor of both PMI and PGI. We propose that such differences in the inhibition properties of 5PAA and 5PAH on the corresponding isomerization reactions catalyzed by PMI and PGI support a catalytic role of the PMI metal cofactor, which is absolutely required for the activity of the enzymes. In contrast, PGI does not use a cofactor. Comparison of our results to the reported inhibition study of rabbit muscle triosephosphate isomerase and yeast class II fructose-1,6-bisphosphate aldolase by their corresponding hydroxamate and carboxylate inhibitors, namely, phosphoglycolohydroxamate and phosphoglycolate (*45*), is quite interesting. Like PGI, triosephosphate isomerase is not metal dependent and is inhibited by both the hydroxamate and carboxylate compounds with binding ratios of 155 and 77 (versus dihydroxyacetone phosphate), respectively. The mechanism of the aldolization reaction catalyzed by the yeast class II aldolase, a zinc-dependent metalloenzyme like PMI, has also been shown to involve an enediolate activated intermediate. In this case, phosphoglycolohydroxamate was reported as a strong inhibitor of the enzyme, while phosphoglycolate did not inhibit the yeast aldolase at all, with binding ratios versus dihydroxyacetone phosphate of 40000 and 0.6, respectively. As for PMI, the reason the carboxylate analogue did not inhibit the zinc aldolase is not clear. However, in the case of the inhibition of the latter enzyme by the hydroxamate analogue, the reported high-resolution crystal structure of *E. coli* class II fructose-1,6-bisphosphate aldolase in complex with phosphoglycolohydroxamate (PDB code 1B57) clearly shows chelation of the catalytic zinc cofactor by the hydroxamate function (*48*). Such similarities in the inhibition of the non-metal-dependent triosephosphate isomerase and PGI, compared to that of the zinc-dependent yeast aldolase and PMI, seem to us quite remarkable. In fact, recent theoretical calculations reported zinc−hydroxamate complexes to be much more stable than the corresponding zinc−carboxylate complexes (*49*). In addition, most of the peptide derivatives reported in the literature as strong inhibitors of the zinc matrix metalloproteinases are hydroxamate derivatives (*50*). Consequently, our inhibition results are consistent with a model for the M6P to F6P isomerization reaction mechanism in which the metal cofactor would behave catalytically rather than structurally (Figure 8), in accord with the initial mechanistic hypothesis reported by Gracy and Noltmann (*51*). While the catalytic base in that model was one of the imidazole groups in the active site, from pK_a measurements, the structural study on PMI from *C. albicans* was not conclusive as to which amino acids are essential to the reaction (*21*). The multistep mechanism can be described as follows: enzyme catalyzed or spontaneous ring opening of the cyclic substrate M6P (step not represented) would first give the open chain form of M6P, which interacts with the

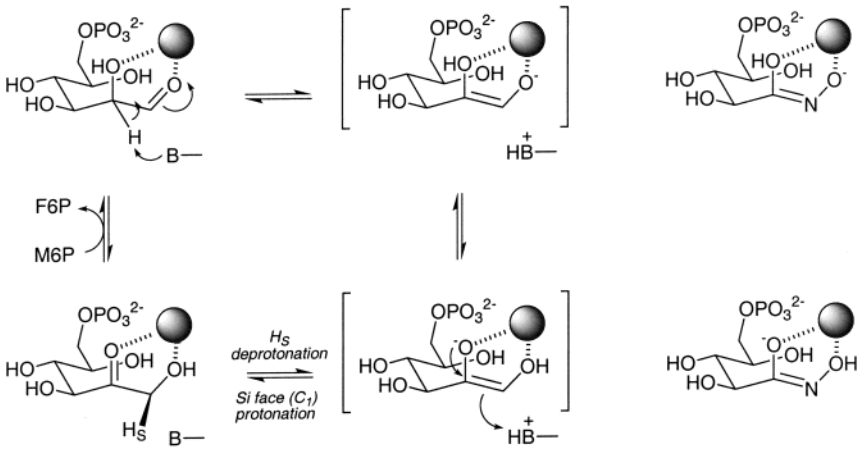

FIGURE 8: Proposed mechanism for the M6P to F6P reversible isomerization catalyzed by PMIs [after Gracy and Noltmann (*51*)] showing a catalytic role for the metal cofactor (represented as a gray circle). Possible structures of the potent inhibitor 5PAH as mimics of the postulated 1,2-*cis*-enediolate high-energy intermediates are depicted to the right of the figure.

active site metal cofactor through its oxygen atoms O1 and O2 (upper left corner of Figure 8). Subsequent polarization of the C2−O2 and C1−O1 bonds by the metal ion acting as a Lewis acid would decrease the pK_a of the C2-H group and facilitate its deprotonation by a nearby basic residue to give the first 1,2-*cis*-enediol or, more likely, a 1,2-*cis*-enediolate reaction intermediate stabilized by the metal ion cofactor. Following a proton transfer between O2 and O1 to give the second 1,2-*cis*-enediolate high-energy intermediate, also stabilized by the metal ion cofactor, protonation on the *si* face of carbon atom C1 by the nearby protonated residue would give the open form of F6P. The open form of F6P thereafter undergoes ring closure to give the final cyclic form of F6P. Another argument in favor of a catalytic role for the metal cofactor is that PMIs are known to have no anomerase or epimerase activity, in contrast to PGI (*52*). Indeed, this could be explained by the coordination of the oxygen atoms O1 and O2 of M6P or F6P to the metal cofactor in the PMI active site, which would prevent rotation of the C1−C2 or C2−C3 bond, respectively.

The postulated forms of the metal ion−5PAH complexes as mimics of the two proposed high-energy intermediates are represented in the right part of Figure 8. The models are in accord, at least for zinc, with theoretical calculations and the experimental three-dimensional X-ray crystal structure of protein complexes containing metal-coordinated hydroxamic acids documented in the Protein Data Bank (*53*). The reason for the unexpected lack of inhibition of yeast and *P. aeruginosa* PMIs by 5PAA is unclear to us. An explanation could be that chelation of the metal cofactor is the driving force of the reaction, rather than the initial binding of the phosphate part of the molecule at the active site. Indeed, we evaluated acetohydroxamate on yeast type I PMI, a compound which bears the hydroxamic functionality but does not supply the sugar portion corresponding to substrate. With an IC_{50} value of 200 μM, acetohydroxamate is a poor inhibitor of yeast PMI. While it confirms that the 5-phospho-D-arabino portion is necessary for strong inhibition, acetohydroxamate is still a better inhibitor than 5PAA by more than 1 order of magnitude. This result would be consistent with the hydroxamate function being involved in the binding to the metal at the active site, as previously reported for the metal-dependent xylose isomerase (*46*). Another hypothesis to explain why 5PAA does not inhibit the PMIs could be that the carboxylate part of the molecule is involved in a highly unfavorable interaction with one of the active site anionic residues, for example, one of the glutamates seen in the reported crystal structure of *C. albicans* PMI (*21*).

Much remains to be done in order to improve our knowledge of the PMI isomerization mechanism. For example, and in contrast to type I PMIs being reported as zinc metalloenzymes, the reason the PMI domain of type II PMIs (PMI/GMPs) does not bind Zn^{2+} specifically is unknown (*27*). This could be highlighted through metal exchange and physicochemical investigations. Undoubtedly, further work, including site-directed mutagenesis and high-resolution diffraction and molecular modeling studies of the PMI−5PAH complexes, should provide important information to address these questions.

REFERENCES

1. Slein, B. W. (1950) Phosphomannose isomerase, *J. Biol. Chem. 186*, 753−761.
2. Malaisse-Lagae, F., Willem, R., Penders, M., and Malaisse, W. J. (1992) Dual anomeric specificity of phosphomannoisomerase assessed by 2D phase sensitive ^{13}C EXSY NMR, *Mol. Cell. Biochem. 115*, 137−142.
3. Rose, I. A., O'Connell, E. L., and Schray, K. J. (1973) Mannose 6-phosphate: anomeric form used by phosphomannose isomerase and its 1-epimerization by phosphoglucose isomerase, *J. Biol. Chem. 248*, 2232−2234.
4. Schray, K. J., Waud, J. M., and Ehrhardt Howell, E. (1978) Phosphomannose isomerase: isomerization of the predicted β-D-fructose 6-phosphate, *Arch. Biochem. Biophys. 189*, 106−108.
5. Payton, M. A., Rheinnecker, M., Klig, L. S., DeTiani, M., and Bowden, E. (1991) A novel *Saccharomyces cerevisiae* secretory mutant possesses a thermolabile phosphomannose isomerase, *J. Bacteriol. 173*, 2006−2010.
6. Smith, D. J., Proudfoot, A. E. I., De Tiani, M., Wells, T. N. C., and Payton, M. A. (1995) Cloning and heterologous expression of the *Candida albicans* gene *PMI 1* encoding phosphomannose isomerase, *Yeast 11*, 301−310.
7. Patterson, J. H., Waller, R. F., Jeevarajah, D., Billman-Jacobe, H., and McConville, M. J. (2003) Mannose metabolism is required for mycobacterial growth, *Biochem. J. 372*, 77−86.
8. Garami, A., and Ilg, T. (2001) The role of the phosphomannose isomerase in *Leishmania mexicana* glycoconjugate synthesis and virulence, *J. Biol. Chem. 276*, 6566−6575.
9. Shinabarger, D., Berry, A., May, T. B., Rothmel, R., Fialho, A., and Chakrabarty, A. M. (1991) Purification and characterization of phosphomannose isomerase-guanosine diphospho-D-mannose pyrophosphorylase, *J. Biol. Chem. 266*, 2080−2088.

10. Panneerselvam, K., Etchison, J. R., and Freeze, H. H. (1997) Human fibroplasts prefers mannose over glucose as a source of mannose for *N*-glycosylation, *J. Biol. Chem. 272*, 23123−23129.
11. De Koning, T. J., Dorland, L., Van Diggelen, O. P., Boonman, A. M. C., De Jong, G. J., Van Noort, W. L., De Schryver, J., Duran, M., Van den Berg, I. E. T., Gerwig, G. J., Berger, R., and Poll-The, B. T. (1998) A novel disorder of *N*-glycosylation due to phosphomannose isomerase deficiency, *Biochem. Biophys. Res. Commun. 245*, 38−42.
12. Jaeken, J., Matthijs, G., Saudubray, J. M., Dionisi-Vici, C., Bertini, E., De Lonlay, P., Henri, H., Carchon, H., Schollen, E., and Van Schaftingen, E. (1998) Phosphomannose isomerase deficiency: a carbohydrate-deficient glycoprotein syndrome with hepatic-intestinal presentation, *Am. J. Hum. Genet. 62*, 1535−1539.
13. Hendriksz, C. J., McClean, P., Henderson, M. J., Keir, D. G., Worthington, V. C., Imtiaz, F., Schollen, E., Matthijs, G., and Winchester, B. G. (2001) Successful treatment of carbohydrate deficient glycoprotein syndrome type Ib with oral mannose, *Arch. Dis. Child. 85*, 339−340.
14. Proudfoot, A. E. I., Turcatti, G., Wells, T. N. C., Payton, M. A., and Smith, D. J. (1994) Purification, cDNA cloning and heterologous expression of human phosphomannose isomerase, *Eur. J. Biochem. 219*, 415−423.
15. Proudfoot, A. E. I., and Payton, M. A. (1994) Purification and characterization of fungal and mammalian phosphomannose isomerases, *J. Protein Chem. 13*, 619−627.
16. Wells, T. N. C., and Payton, M. A. (1994) Inhibition of phosphomannose isomerase by mercury ions, *Biochemistry 33*, 7641−7646.
17. Jensen, S. O., and Reeves, P. R. (1998) Domain organisation in phosphomannose isomerase (types I and II), *Biochim. Biophys. Acta 1382*, 5−7.
18. Wills, E. A., Roberts, I. S., Del Poeta, M., Rivera, J., Casadevall, A., Cox, G. M., and Perfect, J. R. (2001) Identification and characterization of the *Cryptococcus neoformans* phosphomannose isomerase-encoding gene, *MAN1*, and its impact on pathogenicity, *Mol. Microbiol. 40*, 610−620.
19. Gracy, R. W., and Noltman, E. A. (1968) Studies on phosphomannose isomerase I. Isolation, homogeneity measurements, and determination of some physical properties, *J. Biol. Chem. 243*, 3161−3168.
20. Gracy, R. W., and Noltman, E. A. (1968) Studies on phosphomannose isomerase II. Characterization as a zinc metalloenzyme, *J. Biol. Chem. 243*, 4109−4116.
21. Cleasby, A., Wonacott, A., Skarzynski, T., Hubbard, R. E., Davies, G. J., Proudfoot, A. E. I., Bernard, A. R., Payton, M. A., and Wells, T. N. C. (1996) The X-ray crystal structure of phosphomannose isomerase from *Candida albicans* at 1.7 Å resolution, *Nat. Struct. Biol. 3*, 470−479.
22. Papoutsopoulou, S. V., and Kyriakidis, D. A. (1997) Phosphomannose isomerase of *Xanthomonas campestris*: a zinc activated enzyme, *Mol. Cell. Biochem. 177*, 183−191.
23. Ideguchi, T., Hu, C., Kim, B. H., Nishise, H., Yamashita, J., and Kakuno, T. (1993) An open reading frame in the *Rhodospirillum rubrum* plasmid, *pKY1*, similar to *algA*, encoding the bifunctionnal enzyme phosphomannose isomerase-guanosine diphospho-D-mannose pyrophosphorylase (PMI-GMP), *Biochim. Biophys. Acta 1172*, 329−331.
24. Griffin, A. M., Poelwijk, E. S., Morris, V. J., and Gasson, M. J. (1997) Cloning of the *aceF* gene encoding the phosphomannose isomerase and GDP-mannose pyrophosphorylase activities involved in acetan biosynthesis in *Acetobacter xylinum*, *FEMS Microbiol. Lett. 154*, 389−396.
25. Jiang, X. M., Neal, B., Santiago, F., Lee, S. J., Romana, L. K., and Reeves, P. R. (1991) Structure and sequence of the *rfb* (O antigen) gene cluster of *Salmonella serovar typhimurium* (strain LT2), *Mol. Microbiol. 5*, 695−713.
26. Collins, L. V., and Hackett, J. (1991) Sequence of the phosphomannose isomerase-encoding gene of *Salmonella typhimurium*, *Gene 103*, 135−136.
27. Wu, B., Zhang, Y., Zheng, R., Guo, C., and Wang, P. G. (2002) Bifunctional phosphomannose isomerase/GDP-D-mannose pyrophosphorylase is the point of control for GDP-D-mannose biosynthesis in *Helicobacter pylori*, *FEBS Lett. 519*, 87−92.
28. Schmidt, M., Arnold, W., Niemann, A., Kleickmann, A., and Puhler, A. (1992) The *Rhizobium meliloti* pmi gene encodes a new type of phosphomannose isomerase, *Gene 122*, 35−43.
29. Chirgwin, J. M., and Noltmann, E. A. (1975) The enediolate analogue 5-phosphoarabinonate as a mechanistic probe for phosphoglucose isomerase, *J. Biol. Chem. 250*, 7272−7276.
30. Hardré, R., Bonnette, C., Salmon, L., and Gaudemer, A. (1998) Synthesis and evaluation of a new inhibitor of phosphoglucose isomerase: the enediolate analogue 5-phospho-D-arabinohydroxamate, *Bioorg. Med. Chem. Lett. 8*, 3435−3438.
31. Salmon, L., Prost, E., Merienne, C., Hardré, R., and Morgant, G. (2001) A convenient synthesis of aldonhydroxamic acids in water and crystal structure of L-erythronhydroxamic acid, *Carbohydr. Res. 335*, 195−204.
32. Sá-Correia, I., Darzins, A., Wang, S.-K., Berry, A., and Chakrabarty, A. M. (1987) Alginate biosynthetic enzymes in mucoid and nonmucoid *Pseudomonas aeruginosa*: Overproduction of phosphomannose isomerase, phosphomannosemutase, and GDP-mannose pyrophosphorylase by overexpression of the phosphomannose isomerase (*pmi*) gene, *J. Bacteriol. 169*, 3224−3231.
33. Van Schaftingen, E., and Jaeken, J. (1995) Phosphomannomutase deficiency is a cause of carbohydrate-deficient glycoprotein syndrome type I, *FEBS Lett. 377*, 318−320.
34. Noltmann, E. A. (1966) Phosphoglucose isomerase: rabbit muscle (crystalline), *Methods Enzymol. 9*, 557−565.
35. Hardré, R., and Salmon, L. (1999) Competitive inhibitors of yeast phosphoglucose isomerase: synthesis and evaluation of new types of phosphorylated sugars from the synthon D-arabinonolactone-5-phosphate, *Carbohydr. Res. 318*, 110−115.
36. Percheron, F. (1962) Dosage colorimétrique du fructose et des fructofuranosides, *C. R. Hebd. Séances Acad. Sci. 255*, 2521−2522.
37. Zender, R., and Falbriard, A. (1966) Analyse colorimétrique des céto-hexoses et de l'inuline par la réaction à l'acide thiobarbiturique. Conditions de la réaction, *Clin. Chim. Acta 13*, 246−250.
38. Malaisse-Lagae, F., Liemans, V., Yaylali, B., Sener, A., and Malaisse, W. J. (1989) Phosphoglucoisomerase-catalysed interconversion of hexose phosphates; comparison with phosphomannoisomerase, *Biochim. Biophys. Acta 998*, 118−125.
39. Coulin, F., Magnenat, E., Proudfoot, A. E. I., Payton, M. A., Scully, P., and Wells, T. N. C. (1993) Identification of Cys-150 in the active site of phosphomannose isomerase from *Candida albicans*, *Biochemistry 32*, 14139−14144.
40. Wells, T. N. C., Scully, P., and Magnenat, E. (1994) Arginine 304 is an active site residue in phosphomannose isomerase from *Candida albicans*, *Biochemistry 33*, 5772−5782.
41. Rose, I. A., and O'Connell, E. L. (1960) Stereospecificity of the sugar−phosphate isomerase reactions; a uniformity, *Biochim. Biophys. Acta 42*, 159−160.
42. Lee, B. T., and Norman, K. M. (1984) Phosphomannose isomerase and phosphoglucose isomerase in seeds of *Cassia colutoides* and some other legumes that synthesize galactomannan, *Phytochemistry 23*, 983−987.
43. Jaeken, J., Pirard, M., Adamowicz, M., Pronicka, E., and Van Schaftingen, E. (1996) Inhibition of phosphomannose isomerase by fructose 1-phosphate: an explanation for defective *N*-glycosylation in hereditary fructose intolerance, *Pediatr. Res. 40*, 764−766.
44. Hardré, R., Salmon, L., and Opperdoes, F. R. (2000) Competitive inhibition of *Trypanosoma brucei* phosphoglucose isomerase by D-arabinose-5-phosphate derivatives, *J. Enzyme Inhib. 15*, 509−515.
45. Collins, K. D. (1974) An activated intermediate analogue. The use of phosphoglycolohydroxamate as a stable analogue of a transiently occurring dihydroxyacetone phosphate-derived enolate in enzymatic catalysis, *J. Biol. Chem. 249*, 136−142.
46. Allen, K. N., Lavie, A., Petsko, G. A., and Ringe, D. (1995) Design, synthesis and characterization of a potent xylose isomerase inhibitor, D-threonohydroxamic acid, and high-resolution X-ray crystallographic structure of the enzyme−inhibitor complex, *Biochemistry 34*, 3742−3749.
47. Bartlett, P. A., and Marlowe, C. K. (1983) Phosphoramidates as transition state analogue inhibitors of thermolysin, *Biochemistry 22*, 4618−4624.
48. Hall, D. R., Leonard, G. A., Reed, C. D., Watt, C. I., Berry, A., and Hunter, W. N. (1999) The crystal structure of *Escherichia coli* class II fructose-1,6-bisphosphate aldolase in complex with

phosphoglycolohydroxamate reveals details of mechanism and specificity, *J. Mol. Biol. 287*, 383−394.
49. Garmer, D. R., Gresh, N., and Roques, B.-P. (1998) Modeling of inhibitor-metalloenzyme interactions and selectivity using molecular mechanics grounded in quantum chemistry, *Proteins 31*, 42−60.
50. Muri, E. M. F., Nieto, M. J., Sindelar, R. D., and Williamson, J. S. (2002) Hydroxamic acids as pharmaceutical agents, *Curr. Med. Chem. 9*, 1631−1653.
51. Gracy, R. W., and Noltman, E. A. (1968) Studies on phosphomannose isomerase III. A mechanism for catalysis and for the role of zinc in the enzymatic and the nonenzymatic isomerization, *J. Biol. Chem. 243*, 5410−5419.
52. Seeholzer, S. H. (1993) Phosphoglucose isomerase: A ketol isomerase with aldol C2-epimerase activity, *Proc. Natl. Acad. Sci. U.S.A. 90*, 1237−1241.
53. El Yazal, J., and Pang, Y.-P. (2000) Proton dissociation energies of zinc-coordinated hydroxamic acids and their relative affinities for zinc: insight into design of inhibitors of zinc-containing proteinases, *J. Phys. Chem. B 104*, 6499−6504.

BI035688H